J. Fluid Mech. (2014), *vol.* 747, *pp.* 447–459.
doi:10.1017/jfm.2014.180

Linear instability analysis of convection in a laterally heated cylinder

Bo-Fu Wang[1,4], Zhen-Hua Wan[1], Zhi-Wei Guo[2,†], Dong-Jun Ma[3,†] and De-Jun Sun[1,†]

[1]Department of Modern Mechanics, University of Science and Technology of China, Hefei 230027, Anhui, PR China

[2]School of Water Resources and Hydropower Engineering, Wuhan University, Wuhan 430072, Hubei, PR China

[3]National Space Science Center, Chinese Academy of Sciences, Beijing 100190, PR China

[4]School of Power and Mechanical Engineering, Wuhan University, Wuhan 430072, Hubei, PR China

(Received 29 August 2013; revised 23 March 2014; accepted 31 March 2014; first published online 17 April 2014)

The three-dimensional instabilities of axisymmetric flow are investigated in a laterally heated vertical cylinder by linear stability analysis. Heating is confined to a central zone on the sidewall of the cylinder, while other parts of the sidewall are insulated and both ends of the cylinder are cooled. The length of the heated zone equals the radius of the cylinder. For three different aspect ratios, $A = 1.92,\ 2,\ 2.1$ ($A =$ height/radius), the dependence of the critical Rayleigh number on the Prandtl number (from 0.02 to 6.7) has been studied in detail. For such a kind of laterally heated convection, some interesting stability results are obtained. A monotonous instability curve is obtained for $A = 1.92$, while the instability curves for $A = 2$ and $A = 2.1$ are non-monotonous and multivalued. In particular, an instability island has been found for $A = 2$. Moreover, mechanisms corresponding to different instability results are obtained when the Prandtl number changes. At small Prandtl number, the flow is oscillatory unstable, which is dominated by hydrodynamic instability. At intermediate Prandtl number, the interaction between buoyancy and shear in the base flow plays a more important role than pure hydrodynamic instability. At even higher Prandtl number, Rayleigh–Bénard instability becomes the dominant process and the flow loses stability through steady bifurcation.

Key words: buoyancy-driven instability, convection, convection in cavities

1. Introduction

It is well known that crystal growth from bulk melts (Müller & Ostrogorsky 1994; Jaluria 2001) can be greatly influenced by instability due to natural convection. For instance, convective instabilities can result in oscillatory flows that cause inhomogeneity during the crystal growth process (Hurle 1966; Müller 1993). Being one of the most important crystal growth systems in vertical Bridgman growth and vertical zone melting, convection induced in a heated vertical cylinder is usually

† Email addresses for correspondence: juice@mail.ustc.edu.cn, mdj@ustc.edu.cn, dsun@ustc.edu.cn

studied. Three-dimensional instabilities of Rayleigh–Bénard convection were first studied with a relatively simple model, where the fluid contained in vertical cylinders is heated from below. It was shown that the primary instability corresponds to the onset of convection (Charlson & Sani 1970, 1971; Stork & Müller 1975; Buell & Catton 1983) and the secondary instability is connected to axisymmetry-breaking bifurcation (Hardin *et al.* 1990; Neumann 1990; Wanschura, Kuhlmann & Rath 1996; Touihri, Ben Hadid & Henry 1999; Borońska & Tuckerman 2006). The onset of convection is independent of the Prandtl number but dependent on the aspect ratio; however, the stability of axisymmetric flow depends on both the aspect ratio and the Prandtl number. Very recently, Wang *et al.* (2012) performed detailed linear stability analyses for intermediate values of aspect ratio and Prandtl number and concluded that the interaction of the buoyancy mechanism and the inertial mechanism results in complicated instability phenomena.

In practical applications, more realistic heating conditions must be considered for convective flow. For instance, convection in a vertical cylinder that is partially heated from the sidewall and cooled from both upper and lower walls is taken as a typical model, which we also adopt in this study. Here, the length of the heating zone at the mid-height of the cylindrical sidewall is equal to the radius of the cylinder and other parts of the sidewall are insulated. This is especially designed to investigate convection in the vertical zone melting configuration, which is usually employed in industrial applications to carry out the crystal growth process (Selver, Kamotani & Ostrach 1998). It is worth noting that the sidewall heated convection can be induced when any non-zero temperature gradient exists, whereas Rayleigh–Bénard convection is caused by instability of the fluid layer, which is also the essential difference between the two.

Selver *et al.* (1998) experimentally studied convection in a cylinder with a partially heated sidewall. They found that the types of oscillatory transition are strongly dependent on the aspect ratio, including direct transitions or transitions through a first steady bifurcation. Based on the experimental work of Selver *et al.* (1998), Rubinov *et al.* (2004) carefully studied axisymmetric breaking instability of the flow at a fixed Prandtl number $Pr = 0.021$ using two independent numerical approaches. Three different leading modes (mode with the largest growth rate) were found, which interchanged with each other as the aspect ratio was varied. Using the same configuration and Prandtl number, Ma, Henry & BenHadid (2005) studied instability mechanisms numerically at both small and large aspect ratios, and also found hysteresis phenomena with a multiplicity of steady and oscillatory states at intermediate values of the aspect ratio. Furthermore, Erenburg *et al.* (2003) obtained complicated bifurcation diagrams and demonstrated the existence of multiple solutions by studying a two-dimensional model.

Baumgartl *et al.* (1989) performed both a numerical and an experimental study into sidewall heated convection in a configuration similar to the present one, and considered both steady and time-dependent states. However, their work was limited to $A = 1$, and the flow and temperature fields were not studied experimentally in detail. Gelfgat, Bar-Yoseph & Solan (2000) studied stability of axisymmetric flow in a vertical cylinder in which the temperature on the sidewall had a parabolic profile. They presented stability curves for the dependence of critical Rayleigh number on Prandtl numbers in the range $0 \leqslant Pr \leqslant 0.05$ and aspect ratios of $1 \leqslant A \leqslant 5$. Instability mechanisms were also evaluated. Subsequently, Gemeny, Martin Witkowski & Walker (2007) extended the linear stability analysis of Gelfgat *et al.* (2000) to the flux condition and found that the two kinds of thermal boundary conditions gave radically different results.

Previous studies have demonstrated that the stability properties of convective flows are strongly dependent on the geometry and the Prandtl number (Braunsfurth & Mullin 1996; Gelfgat, Bar-Yoseph & Yarin 1997, 1999). A strong dependence on variation of the heating conditions can also be reasonably expected. As shown in Wang *et al.* (2012) for cylindrical Rayleigh Bénard models, the stability properties of a given flow cannot be completely understood without a detailed exploration in parametric space. In particular, stability properties under moderate control parameters should be paid more attention where interactions among several instability mechanisms occur.

In this paper, we address the stability of axisymmetric convection in a cylinder with a partially heated sidewall. The dependence of the critical Rayleigh number on Prandtl numbers in the range $0.02 \leqslant Pr \leqslant 6.7$ and for aspect ratios of $A = 1.92, 2, 2.1$ are mainly studied. Comparisons of the present results with those of Rayleigh–Bénard convection in a cylinder are also made.

2. Governing equations and numerical methods

We consider an incompressible Newtonian fluid confined in a vertical cylindrical cavity of aspect ratio $A = H/R$, where H is the height and R is the radius of the cavity. The cylinder is partially heated from the central part of the sidewall with a uniformly distributed high temperature T_h, and both ends of the cylinder are cooled with a uniformly distributed low temperature T_c, whereas the region above and below the heated zone at the sidewall is adiabatic. In cylindrical coordinates, the domain has a size of $(r, \varphi, z) \in [0, 1] \times [0, 2\pi] \times [0, A]$. For the current geometry, the meridional plane has the configuration shown in figure 1. The three-dimensional problem is described by the Oberbeck–Boussinesq equations (Oberbeck 1879; Boussinesq 1903). All the physical characteristics are taken as constant, apart from the density, which is taken as a linear function of temperature in the buoyancy term, $\rho = \rho_0[1 - \alpha(T - T_0)]$, where α is the thermal expansion coefficient and T_0 is the reference temperature ($T_0 = T_c$). The length, time, velocity and pressure are scaled by R, R^2/κ, κ/R and $\rho\ (\kappa/R)^2$, respectively, where κ is the thermal diffusivity. The non-dimensional temperature is defined by $\Theta = (T - T_c)/(T_h - T_c)$. The final dimensionless governing equations can be written as

$$\nabla \cdot \boldsymbol{u} = 0, \tag{2.1}$$

$$\frac{\partial \boldsymbol{u}}{\partial t} + \boldsymbol{u} \cdot \nabla \boldsymbol{u} = -\nabla p + Pr\, \nabla^2 \boldsymbol{u} + PrRa\Theta \hat{\boldsymbol{z}}, \tag{2.2}$$

$$\frac{\partial \Theta}{\partial t} + \boldsymbol{u} \cdot \nabla \Theta = \nabla^2 \Theta, \tag{2.3}$$

where $Pr = \nu/\kappa$ is Prandtl number, ν is kinematic viscosity, $Ra = g\alpha(T_h - T_c)R^3/(\kappa\nu)$ is the Rayleigh number, g is the gravitational acceleration, and $\hat{\boldsymbol{z}}$ is a unit vector in the z direction.

The boundary conditions for velocity and temperature are

$$\boldsymbol{u} = 0 \quad \text{for } r = 1 \text{ or } z = 0, A, \tag{2.4}$$

$$\frac{\partial \Theta}{\partial r} = 0 \quad \text{for } r = 1,\ z < \frac{A}{2} - \frac{1}{2} \text{ or } z > \frac{A}{2} + \frac{1}{2}, \tag{2.5}$$

$$\Theta = 1 \quad \text{for } \frac{A}{2} - \frac{1}{2} \leqslant z \leqslant \frac{A}{2} + \frac{1}{2}, \tag{2.6}$$

$$\Theta = 0 \quad \text{for } z = 0 \text{ and } z = A. \tag{2.7}$$

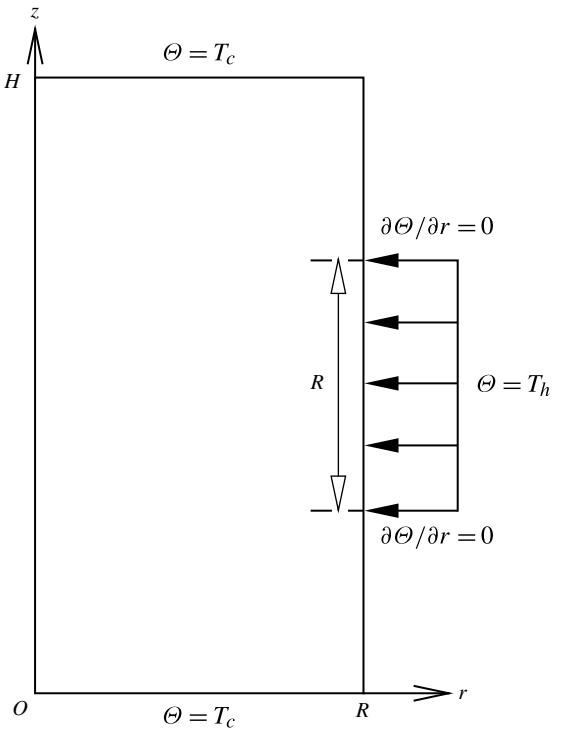

FIGURE 1. Geometry of the problem: the cylindrical wall is partially heated from the side.

The solutions of the governing equations (2.1)–(2.3) and boundary conditions (2.4)–(2.7) are obtained by using a second-order fractional-step algorithm in cylindrical coordinates (Verzicco & Orlandi 1996) which has been employed in our previous studies (Ma *et al.* 2005; Ma, Sun & Yin 2006; Wang *et al.* 2012).

The linear stability analysis is performed in two steps: first, a steady solution is obtained by solving the Navier–Stokes equations using the Jacobian-free Newton–Krylov (JFNK) (Knoll & Keyes 2004) method, then the eigenmodes of the Navier–Stokes equations linearized about this base flow are computed using the Arnoldi algorithm from the ARPACK library (Tuckerman & Barkley 2000). The linearized Navier–Stokes equations are

$$\partial_t \boldsymbol{u}' = (\boldsymbol{N}_{\boldsymbol{u}} + \boldsymbol{L})\boldsymbol{u}'. \tag{2.8}$$

The correspondingeigenequations are $(\boldsymbol{N}_{\boldsymbol{u}} + \boldsymbol{L})\boldsymbol{u}' = \lambda \boldsymbol{u}'$, where $\boldsymbol{J} = (\boldsymbol{N}_{\boldsymbol{u}} + \boldsymbol{L})$ is the Jacobian matrix. If its eigenvalues λ_j and corresponding eigenvectors ϕ_j are found, the stability of the steady solution $\boldsymbol{u}$ is determined by the three-dimensional global modes $\phi_j(x, y, z)\exp(\lambda_j t)$, $j = 1, \ldots, n$. The temporal growth rate is given by the real part $\lambda_{j,r}$ and the frequency by the imaginary part $\lambda_{j,i}$.

The implicitly restarted Arnoldi method (Lehoucq, Sorensen & Yang 1998) using the ARPACK routines is implemented to calculate the leading eigenvalues. By time-stepping the linearized equations, we are able to construct a small matrix which represents the action of the Jacobian $\boldsymbol{J}$ on the subspace of leading eigenvectors. Diagonalization of this matrix gives the leading eigenvalues and eigenvectors.

Our code has been successfully tested by comparison with the results of Buell & Catton (1983), Touihri *et al.* (1999) and Borońska & Tuckerman (2006) for instability analysis of Rayleigh–Bénard convection in a cylinder (Ma *et al.* 2006; Wang *et al.* 2012). In addition, our code has also been verified by comparison with the results of Selver *et al.* (1998), Gelfgat *et al.* (2000) and Rubinov *et al.* (2004) for convection in a sidewall heated cylinder (Ma *et al.* 2005). The simulations in the present research have been performed using a $60 \times 60 \times 140$ grid in the radial, azimuthal and vertical directions, respectively. A non-uniform mesh is utilized in the radial and axial directions, with mesh points clustered toward the boundaries.

3. Results

3.1. *Stability results*

Before performing linear stability analysis, the steady solution should first be obtained. Currently, for all base flows, the heated fluid rises along, and close to the sidewall it and then descends along the cylinder axis. The toroidal roll occupies almost the whole cylinder. In the lower part of the cylinder the fluid is stably stratified, while the fluid is unstably stratified in the upper part. It is shown that the two stratifications in the sidewall heated cylinder play an important role in flow instability and may lead to a multiplicity of flow patterns (Selver *et al.* 1998; Gelfgat *et al.* 2000; Rubinov *et al.* 2004). On increasing the Rayleigh number beyond a critical value $Ra_{cr}(Pr)$, the base flow undergoes an axisymmetry breaking bifurcation and becomes a three-dimensional flow. Depending on Pr, the base flow may undergo either oscillatory or steady bifurcation. Stabilities have been explored comprehensively for $0.02 \leqslant Pr \leqslant 6.7$ when the aspect ratio equals 1.92, 2 and 2.1, respectively.

Stability curves indicating the dependence of the critical Rayleigh number on the Prandtl number for three fixed values of aspect ratio are shown in figure 2. Qualitative and quantitative differences are observed in certain ranges of Prandtl number. For clarity, the range of Prandtl number is divided into three regions. The first region of Prandtl numbers is from $Pr = 0.02$ to approximately 0.1. The stability properties are very similar for all three aspect ratios in this interval. The modes with the largest growth rate are all oscillatory with azimuthal wavenumber $m = 2$. The critical Rayleigh number increases quickly with increasing Pr, with values close to each other for the three aspect ratios. The second region is from approximately $Pr = 0.1$ to 2.5. The axisymmetric base flow loses stability and becomes a steady $m = 4$ flow at Rayleigh numbers greater than 10^4 for $A = 1.92$, as shown in figure 2(*a*). A similar result is found for $A = 2$, as shown in figure 2(*b*), where the instability mode is a steady $m = 3$ flow for intermediate values of the Prandtl number. Besides, the axisymmetric base flow loses stability to a steady $m = 1$ flow at lower Rayleigh numbers of $2550 < Ra < 4050$. The critical points corresponding to $m = 1$ modes form a closed curve, which presents an instability island. The stability curve for $A = 2.1$ behaves quite differently from the previous two cases. The values of critical Rayleigh number have dropped below 2000 for intermediate values of the Prandtl number ($0.27 \leqslant Pr \leqslant 0.84$), as shown in figure 2(*c*). The mode with the highest growth rate is a steady $m = 1$ mode. The stability diagrams in the Prandtl number ranges $0.1 < Pr < 0.27$ and $0.84 < Pr < 2.5$ show 'S' and anti-'S' shapes, respectively. The third region is from approximately $Pr = 2.5$ to 6.7. Much simpler critical curves are obtained in this Prandtl number interval. The critical Rayleigh number increases with increasing Prandtl number and the critical modes are all steady. The azimuthal wavenumber for the mode with the largest growth rate is $m = 5$ for $A = 1.92$ and $m = 4$ for $A = 2$ and 2.1.

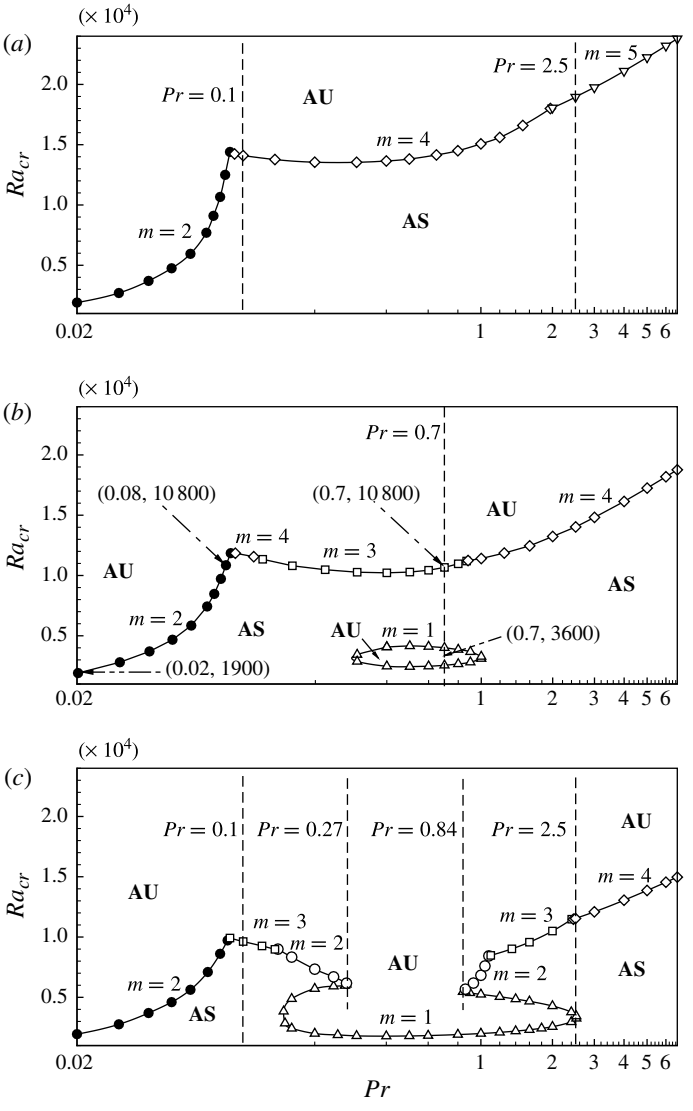

FIGURE 2. Stability curves for three-dimensional instability of axisymmetric basic flow: (*a*) $A = 1.92$, (*b*) $A = 2$, (*c*) $A = 2.1$. The range of Prandtl numbers is $0.02 \leqslant Pr \leqslant 6.7$. Solid curves with hollow symbols represent steady transitions and filled symbols oscillatory transitions. Up triangles (△) indicate $m = 1$ modes at the transition, circles (○) $m = 2$ modes, squares (□) $m = 3$ modes, diamonds (◇) $m = 4$ modes, down triangles (▽) $m = 5$ modes and filled circles (●) $m = 2$ modes. AS in the figures indicates regions in which the axisymmetric flow is stable, while AU indicates there is no stable axisymmetric base flow in the region.

Figure 2 demonstrates the variation of the stability curves with aspect ratio and has some general features. The critical Rayleigh number decreases as the aspect ratio is increased. In the region of moderate Prandtl number and low Rayleigh number, an instability island gradually appears with increasing aspect ratio. The instability region grows larger with a further increase in aspect ratio, until the upper boundary of the

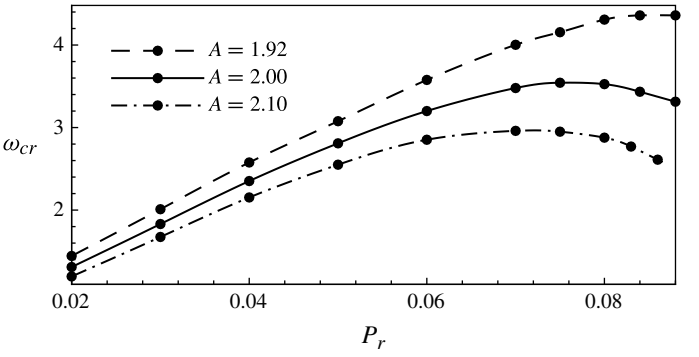

FIGURE 3. Critical frequency ω_{cr} versus the Prandtl number. Filled circles (•) indicate $m = 2$ modes at the transition.

region encounters the stability curve at high Rayleigh number and a concave curve is obtained. When the aspect ratio is larger than $A = 2.1$, a monotonous stability curve with relatively low critical Rayleigh number is expected. As observed in other cylindrical thermal convection configurations (Gelfgat *et al.* 2000; Wang *et al.* 2012), the existence of a multivalued stability curve depends strongly on the aspect ratio and Prandtl number.

Figure 3 presents the dependence of the critical angular frequency on the Prandtl number. It is observed that the frequencies increase as Pr increases for $A = 1.92$. However, for $A = 2$ and $A = 2.1$, the frequencies increase at first to a maximum value and then decrease with increasing Pr. The frequencies for cylinders with smaller aspect ratios are a little higher than those for cylinders with larger aspect ratios.

The dependence of the critical Rayleigh number on the aspect ratio for the fixed Prandtl number $Pr = 0.6$ is shown in figure 4. The modes with the largest growth rate are all steady. The axisymmetric flow loses stability to $m = 3$ or $m = 4$ flow at relatively high Rayleigh number, to $m = 2$ flow at intermediate Rayleigh number and to $m = 1$ flow at low Rayleigh number. The stability curve exhibits an anti-'S' shape. There are three critical Rayleigh numbers for a fixed aspect ratio in the narrow interval $1.98 < A < 2.07$. The stability diagram of the variation of critical Rayleigh number with Prandtl number for a fixed aspect ratio in this interval may contain closed instability curves. Figure 4 shows that flow instability in a partially heated sidewall cylindrical convection is very sensitive to variations in the aspect ratio – a reduction of 0.1 in the aspect ratio leads to a reduction of the critical Rayleigh number by approximately 10^4. Multivalued stability curves can be observed only for a certain range of aspect ratio.

The structures of the modes with the largest growth rates can be used to gain some additional understanding as to how the instability sets in. The three-dimensional flow patterns beyond the axisymmetric break bifurcation are characterized by the mode with the largest growth rate, which are defined by the eigenvectors of the linearized stability problem. Some of the perturbation distributions in the cylinder corresponding to different control parameters and equal azimuthal wavenumber are similar, but most of them are not. Figure 5 shows four characteristic patterns of the temperature perturbations obtained in the present study. Two perturbation patterns corresponding to the transition from axisymmetric to periodic three-dimensional flow due to the Hopf bifurcation are shown in figures 5(*a*) and 5(*b*). The critical

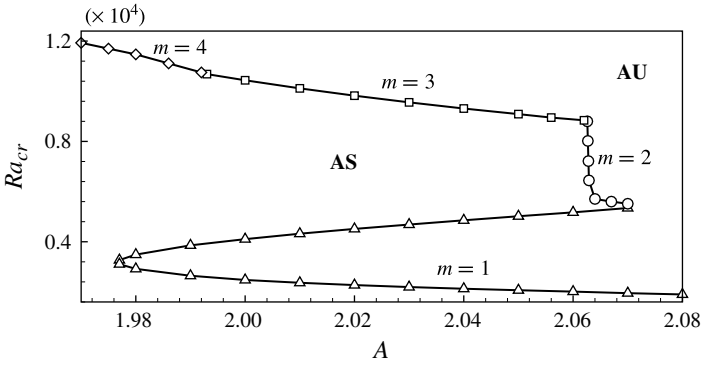

FIGURE 4. Critical Rayleigh number Ra_{cr} as a function of aspect ratio A for $Pr = 0.6$. Solid curves with hollow symbols represent steady transitions. Up triangles (△) indicate $m = 1$ modes at the transition, circles (○) $m = 2$ modes, squares (□) $m = 3$ modes and diamonds (◇) $m = 4$ modes. AS in the figure indicates regions in which the axisymmetric flow is stable, while AU indicates there is no stable axisymmetric base flow in the region.

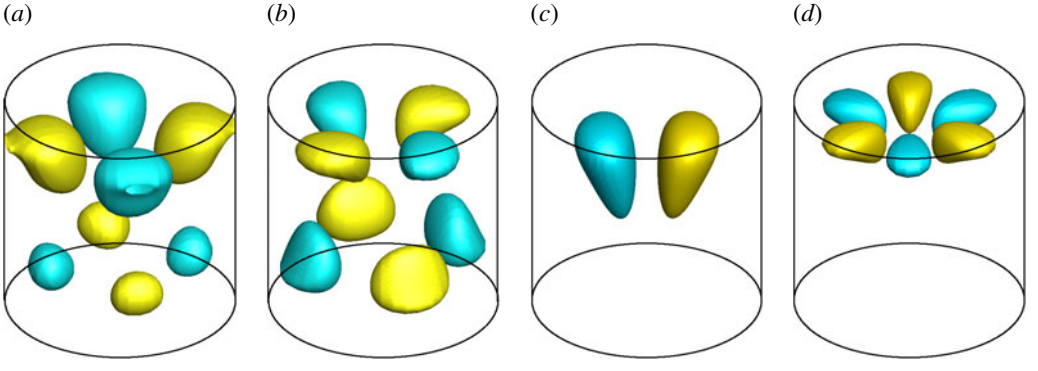

FIGURE 5. (Colour online) Isosurfaces of the temperature perturbations for (*a*) $(Pr, Ra) = (0.02, 1900)$, (*b*) $(Pr, Ra) = (0.08, 10\,800)$, (*c*) $(Pr, Ra) = (0.7, 3600)$, (*d*) $(Pr, Ra) = (0.7, 10\,800)$. The two isovalues plotted in each figure are the half-maximum (green) and the half-minimum (yellow) of the temperature perturbation.

angular frequencies are 1.31 and 3.41, respectively. Large amplitude oscillations are distributed in most parts of the cylinder. The stronger oscillations are located in the higher part of the cylinder for $(Pr, Ra) = (0.02, 1900)$ and in the lower part of the cylinder for $(Pr, Ra) = (0.08, 10\,800)$. The oscillatory instability is dominated by hydrodynamics and may be associated with instability of the circulating flow. Two perturbation patterns corresponding to the transition from axisymmetric to steady three-dimensional flow at large values of the Prandtl number due to steady bifurcations are shown in figures 5(*c*) and 5(*d*). The critical wavenumbers are $m = 1$ and $m = 3$, respectively. The strongest perturbations are located inside the unstably stratified fluid layer for $(Pr, Ra) = (0.7, 10\,800)$ (see figure 5*d*). This steady instability is related to Rayleigh–Bénard instability of the unstably stratified layer. The strongest perturbations are located in the upper half of the cylinder for $(Pr, Ra) = (0.7, 3600)$ (see figure 5*c*), where interaction of the unstably stratified layer with the heated flow region is expected.

3.2. *Energy analysis*

In order to get some physical insight into the transition to three-dimensional flow, energy analyses are usually performed (Wanschura *et al.* 1996; Ma *et al.* 2005; Wang *et al.* 2012). The perturbation kinetic energy is defined by integrating over the volume Ω occupied by the fluid:

$$K = \int_{\Omega} \tfrac{1}{2}\boldsymbol{u}'\boldsymbol{u}'\mathrm{d}\Omega. \tag{3.1}$$

Close to the threshold, a Reynolds–Orr equation can then be written for the rate of change of the total perturbationkinetic energy:

$$\frac{\mathrm{d}K}{\mathrm{d}t} = K_v + K_d + K_b \tag{3.2}$$

where

$$\begin{aligned} K_v &= \int_{\Omega} \left(u_r'u_r'\frac{\partial u_r}{\partial r} + u_r'u_z'\frac{\partial u_r}{\partial z} + u_z'u_r'\frac{\partial u_z}{\partial r} + u_z'u_z'\frac{\partial u_z}{\partial z} + \frac{u_\varphi'u_\varphi'u_r}{r} \right) \mathrm{d}\Omega \\ &= K_{v1} + K_{v2} + K_{v3} + K_{v4} + K_{v5} \end{aligned} \tag{3.3}$$

$$K_d = -Pr \int_{\Omega} (\nabla \times \boldsymbol{u}')^2 \mathrm{d}\Omega \tag{3.4}$$

$$K_b = PrRa \int_{\Omega} u_z'\Theta' \mathrm{d}\Omega \tag{3.5}$$

K_v represents the production of perturbation energy by shear of the base flow, while K_d and K_b represent the viscous dissipation of the perturbation kinetic energy and buoyancy forces, respectively. The calculation of these terms enables us to evaluate which term contributes more to the perturbation energy growth. Terms on the right-hand side of (3.2) with a positive (negative) sign denote destabilization (stabilization) of the base flow. The sign and magnitude of K_v depends sensitively on both the critical mode and the basic state – both effects of stabilization and destabilization are included. As K_d is negative, it is stabilizing and $|K_d|$ is used for normalization.

The instability mechanism at low values of of the Prandtl number ($Pr = 0.021$) for sidewall heated natural convection has been investigated by Gelfgat *et al.* (2000) and Rubinov *et al.* (2004) through eigenperturbation analysis, and by Ma *et al.* (2005) through perturbation kinetic energy analysis. They concluded that the oscillatory axisymmetric instability is mainly caused by an inertial mechanism, but that it is affected by the Rayleigh–Bénard mechanism as well. Instability at high values of Prandtl number ($Pr > 1$) is obviously dominated by the Rayleigh–Bénard mechanism. Here, we focus on studying instability mechanisms at intermediate values of Prandtl number, where the stability curve is multivalued.

The kinetic perturbation energy transfer budget has been performed for $Pr = 0.7$ and $A = 2$, where there are three critical Rayleigh numbers ($Ra_{cr1} = 2553$, $Ra_{cr2} = 4005$ and $Ra_{cr3} = 10\,670$). Figure 6(*a*) shows the result given by the energy analysis for $2000 < Ra < 4800$. The rate of change of kinetic perturbation energy is positive for $2553 < Ra < 4005$, at first increasing with increasing Rayleigh number, then decreasing as the Rayleigh number further increases. This corresponds to processes of destabilization and stabilization of the axisymmetric flow, respectively. As can be seen from the figure, the buoyancy term K_b and inertial terms $K_{v1}, K_{v3}, K_{v4}, K_{v5}$ are all destabilizing and their values are all increasing for a Rayleigh number around 2553,

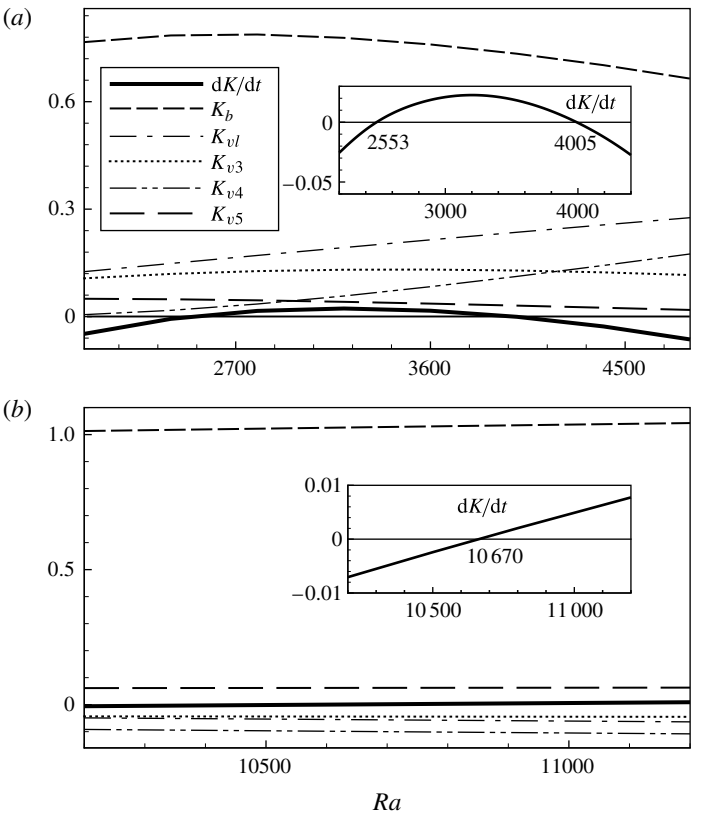

FIGURE 6. Perturbation kinetic energy contributions at a fixed Prandtl number $Pr = 0.7$ for (*a*) $A = 2$, $2000 \leqslant Ra \leqslant 4800$ and (*b*) $A = 2$, $10\,200 \leqslant Ra \leqslant 11\,200$.

being responsible for the instability. The term K_{v2} is very small (close to zero), thus it is not plotted in the figure. The value of the viscous term K_d is always negative and it is not plotted either. As the inertial terms K_{v1} and K_{v4} increase with Rayleigh number, whereas K_{v3} and K_{v5} change only slightly, the decrease of the buoyancy term K_b leads to stabilization of the base flow. Here, K_{v1} measures the amplification of the radial velocity disturbance (u_r') by radial gradients of the basic radial flow ($\partial_r u_r$) and K_{v4} describes the amplification of the axial velocity disturbance (u_z') by axial gradients of the basic axial flow ($\partial_z u_z$). Increasing the Rayleigh number intensifies the horizontal temperature gradient, which would lead to an increase in K_{v1}, consequently, K_{v4} would be increased due to the continuity requirement. The reduction of vertical unstable stratification would induce a stabilization effect. Figure 6(*b*) shows the energy analysis for $10\,200 < Ra < 11\,200$. It can be seen in the figure that the flow bifurcation is caused by the buoyancy effect. The destabilizing terms (K_{v1}, K_{v3}, K_{v4}) at low Rayleigh number play a stabilizing role.

Here, we compare the present result with that of cylindrical Rayleigh–Bénard convection (Wang *et al.* 2012). In the Rayleigh–Bénard configuration, multivalued stability curves have also been found in a moderate parameter region, including a closed curve encircling an area for stable axisymmetric flow. Combination of the buoyancy term and the inertial term (K_{v2} and K_{v3}) would promote energy growth. The instability mechanism for laterally heated convection under moderate control

parameters shown in figure 6 is also due to the combined action of buoyancy and inertial mechanisms. However, the major contribution to inertial terms is replaced by K_{v1} and K_{v4} as a result of a lateral temperature gradient.

The competition between buoyancy and shear may lead to complex phenomena. One typical example is pattern formation in inclined layer convection (Daniels, Plapp & Bodenschatz 2003; Daniels *et al.* 2008), where the phase space is divided into several regions of characteristic behaviour which is caused by different degrees of combination of the two mechanisms. In addition, competition between centrifugal and shear instability may lead to similar results, as has been found in spiral Couette flow (Meseguer & Marques 2000), spiral Poiseuille flow (Meseguer & Marques 2002), spiral Couette flow with a Bingham-plastic fluid (Peng & Zhu 2004) and Taylor–Couette flow with a radial temperature gradient (Chen *et al.* 2006). These studies provide a common result that an instability island can be found in their marginal stability curves. Consequently, it is believed such a kind of instability property is universal in the flow under the conditions of competition between two instability mechanisms.

4. Conclusion

In this paper, we have studied the stability of steady axisymmetric convection in a vertical cylinder with a partially heated sidewall. The temperature distribution of the base flow results in an unstable stratified layer, a stable stratified layer and a laterally stratified layer. The stability analysis shows that the critical Rayleigh number, as well as the critical frequency of oscillation and the critical azimuthal wavenumber, depends strongly on the Prandtl number and aspect ratio. At low values of Prandtl number, the basic state loses its stability due to hydrodynamic instability combining with the buoyancy effect. At high values of Prandtl number, the flow instability is mainly induced by buoyancy. At moderate Prandtl number, the combination of the buoyancy mechanism and the inertial mechanism lead to a multivalued stability curve, and the dominant inertial terms contributed are the radial gradient of the radial velocity (K_{v1}) and the axial gradient of the axial velocity (K_{v4}). This is attributed to a horizontal temperature gradient, which is different from the multivalued instability found in cylindrical Rayleigh–Bénard convection (Wang *et al.* 2012). The flow stability also depends strongly on boundary conditions (Barwölff, König & Seifert 1997; Gemeny *et al.* 2007). Therefore, the boundary conditions and values of the control parameters should be as precise as possible in order to determine the critical values. In particular, in practical applications, the mathematical models employed are usually insufficient to describe the flow process precisely; hence, a detailed parametric study is of great significance for a full understanding of flow instability.

Acknowledgements

This work was supported by the National Natural Science Foundation of China under Grant No. 11232011, and the 111 Project of China under Grant No. B07033.

REFERENCES

Barwölff, G., König, F. & Seifert, G. 1997 Thermal buoyancy convection in vertical zone melting configurations. *J. Appl. Math. Mech.* **10**, 757–766.

Baumgartl, J., Budweiser, W., Mueller, G. & Neumann, G. 1989 Studies of buoyancy driven convection in a vertical cylinder with parabolic temperature profile. *J. Cryst. Growth* **97**, 9–17.

BOROŃSKA, K. & TUCKERMAN, L. S. 2006 Standing and travelling waves in cylindrical Rayleigh–Bénard convection. *J. Fluid Mech.* **559**, 279–298.

BOUSSINESQ, J. 1903 *Théorie Analytique de la Chaleur*, vol. 2. Gauthier–Villars.

BRAUNSFURTH, M. G. & MULLIN, T. 1996 An experimental study of oscillatory convection in liquid gallium. *J. Fluid Mech.* **327**, 199–219.

BUELL, J. C. & CATTON, I. 1983 The effect of wall conduction on the stability of a fluid in a right circular cylinder heated from below. *Trans. ASME J. Heat Transfer* **105**, 255–260.

CHARLSON, G. S. & SANI, R. L. 1970 Thermoconvective instability in a bounded cylindrical fluid layer. *Intl J. Heat Mass Transfer* **13**, 1479–1496.

CHARLSON, G. S. & SANI, R. L. 1971 On thermoconvective instability in a bounded cylindrical fluid layer. *Intl J. Heat Mass Transfer* **14**, 2157–2160.

CHEN, J. G., CHEN, H. X., ZHANG, G. H. & FU, S. 2006 Stability of flow between rotating cylinders with axial buoyancy effect. *Sci. China Phys. Mech. Astron.* **49**, 564–575.

DANIELS, K. E., BRAUSCH, O., PESCH, W. & BODENSCHATZ, E. 2008 Competition and bistability of ordered undulations and undulation chaos in inclined layer convection. *J. Fluid Mech.* **597**, 261–282.

DANIELS, K. E., PLAPP, B. B. & BODENSCHATZ, E. 2003 Pattern formation in inclined layer convection. *Phys. Rev. Lett.* **84**, 5320–5323.

ERENBURG, V., GELFGAT, A. YU., KIT, E., BAR-YOSEPH, P. Z. & SOLAN, A. 2003 Multiple states, stability and bifurcations of natural convection in a rectangular cavity with partially heated vertical walls. *J. Fluid Mech.* **492**, 63–89.

GELFGAT, A. YU., BAR-YOSEPH, P. Z. & SOLAN, A. 2000 Axisymmetry breaking instabilities of natural convection in a vertical Bridgman growth configuration. *J. Cryst. Growth* **220**, 316–325.

GELFGAT, A. YU., BAR-YOSEPH, P. Z. & YARIN, A. L. 1997 On oscillatory instability of convective flows at low Prandtl number. *Trans. ASME J. Fluids Engng.* **119**, 823–830.

GELFGAT, A. YU., BAR-YOSEPH, P. Z. & YARIN, A. L. 1999 Stability of multiple steady states of convection in laterally heated cavities. *J. Fluid Mech.* **388**, 315–334.

GEMENY, L. E., MARTIN WITKOWSKI, L. & WALKER, J. S. 2007 Buoyant instability in a laterally heated vertical cylinder. *Intl J. Heat Mass Transfer* **50**, 1010–1017.

HARDIN, G. R., SANI, R. L., HENRY, D. & ROUX, B. 1990 Buoyancy-driven instability in a vertical cylinder: Binary fluids with Soret effect. Part 1. General-theory and stationary stability results. *Intl J. Numer. Meth. Fluids* **10** (1), 79–117.

HURLE, D. T. J. 1966 Temperature oscillations in molten metals and their relationship to growth striae in melt-grown crystals. *Phil. Mag.* **13**, 305–310.

JALURIA, Y. 2001 Fluid flow phenomena in materials processing: the 2000 Freeman scholar lecture. *Trans. ASME J. Fluids Engng.* **123**, 173–210.

KNOLL, D. A. & KEYES, D. E. 2004 Jacobian-free Newton–Krylov methods: a survey of approaches and applications. *J. Comput. Phys.* **193**, 357–397.

LEHOUCQ, R. B., SORENSEN, D. C. & YANG, C. (Eds.) 1998 *ARPACK Users Guide: Solution of Large-Scale Eigenvalue Problems with Implicitly Restarted Arnoldi Methods*. SIAM.

MA, D. J., HENRY, D. & BENHADID, H. 2005 Three-dimensional numerical study of natural convection in vertical cylinders partially heated from the side. *Phys. Fluids* **17**, 124101.

MA, D. J., SUN, D. J. & YIN, X. Y. 2006 Multiplicity of steady states in cylindrical Rayleigh–Bénard convection. *Phys. Rev.* E **74**, 037302.

MESEGUER, A. & MARQUES, F. 2000 On the competition between centrifugal and shear instability in spiral Couette flow. *J. Fluid Mech.* **402**, 33–56.

MESEGUER, A. & MARQUES, F. 2002 On the competition between centrifugal and shear instability in spiral Poiseuille flow. *J. Fluid Mech.* **455**, 129–148.

MÜLLER, G. 1993 Convective instabilities in melt growth configurations. *J. Cryst. Growth* **128**, 26–36.

MÜLLER, G. & OSTROGORSKY, A. 1994 Convection in melt growth. In *Handbook of Crystal Growth* (ed. D. T. J. Hurle), vol. 2, pp. 711–781. North-Holland.

NEUMANN, G. 1990 Three-dimensional numerical simulation of buoyancy-driven convection in vertical cylinders heated from below. *J. Fluid Mech.* **214**, 559–578.

OBERBECK, A. 1879 Über die Wärmeleitung der Flüssigkeiten bei Berücksichtigung der Strömungen infolge von Temperaturdifferenzen. *Ann. Phys. Chem.* **7**, 271–292.

PENG, J. & ZHU, K. Q. 2004 Linear stability of Bingham fluids in spiral Couette flow. *J. Fluid Mech.* **512**, 21–45.

RUBINOV, A., ERENBURG, V., GELFGAT, A. YU., KIT, E., BAR-YOSEPH, P. Z. & SOLAN, A. 2004 Three-dimensional instabilities of natural convection flow in a vertical cylinder with partially heated sidewall. *Trans. ASME J. Heat Transfer* **126**, 586–599.

SELVER, R., KAMOTANI, Y. & OSTRACH, S. 1998 Natural convection of a liquid metal in vertical cylinders heated locally from the side. *Trans. ASME J. Heat Transfer* **120**, 108–114.

STORK, K. & MÜLLER, U. 1975 Convection in boxes: an experimental investigation in vertical cylinders and annuli. *J. Fluid Mech.* **71**, 231–240.

TOUIHRI, R., BEN HADID, H. & HENRY, D. 1999 On the onset of convective instabilities in cylindrical cavities heated from below. I. Pure thermal case. *Phys. Fluids* **11**, 2078–2088.

TUCKERMAN, L. S. & BARKLEY, D. 2000 Bifurcation analysis for time-steppers. In *Numerical Methods for Bifurcation Problems and Large-Scale Dynamical Systems* (ed. E. Doedel & L. S. Tuckerman), vol. 119, pp. 453–466. Springer.

VERZICCO, R. & ORLANDI, P. 1996 A finite-difference scheme for the three-dimensional incompressible flows in cylindrical coordinates. *J. Comput. Phys.* **123**, 402–414.

WANG, B. F., MA, D. J., CHEN, C. & SUN, D. J. 2012 Linear stability analysis of cylindrical Rayleigh–Bénard convection. *J. Fluid Mech.* **38**, 27–39.

WANSCHURA, M., KUHLMANN, H. C. & RATH, H. J. 1996 Three-dimensional instability of axisymmetric buoyant convection in cylinders heated from below. *J. Fluid Mech.* **326**, 399–415.